JOURNAL OF MATERIALS SCIENCE 27 (1992) 1149–1156

Interfacial reactions between thin metal films and polar {0001} oriented CdS substrates

Part II *Copper and gold films on CdS*

E. K. CHIEH, Z. A. MUNIR
Division of Materials Science and Engineering, University of California, Davis, CA 95616, USA

The interaction between thin films of copper and gold and polar {0001} substrates of CdS was investigated. The out-diffusion of sulphur into the copper film resulted in a broad interface, but because of relatively weak sulphur–copper bonding, chemical trapping was not observed. For both cases (Cu–CdS and Au–CdS) no difference in behaviour was observed between the A (0001) and B ($000\bar{1}$) oriented CdS substrates. The non-stoichiometric out-diffusion of the substrate components (S and Cd) into the Cu, Au, and Al was similar to the case when III–V compounds were the substrates. The dependence of the Cd/S concentration ratio on metal film thickness showed a clear division between reactive and non-reactive metals.

1. Introduction

The redistribution of charge across a metal–semiconductor interface results in the creation of a dipole. The magnitude and sign of this dipole depends on the interaction between the metal and the semiconductor, and its existence can influence atomic mobilities across the interface. The nature of the interaction between the metal and the semiconductor depends, in part, on the reactivity of the metal. In a preceding paper [1] we reported results on the case of a reactive metal (aluminium) deposited on polar {0001} faces of CdS. In this paper we report similar results for the cases of copper and gold deposited on the polar surfaces. The two cases reported here will represent examples of a moderately reactive and a non-reactive metal. Brillson and co-workers [2–6] have provided considerable information on the nature of interactions between metals and III–V and II–VI semiconductors, as discussed in detail in the previous paper [1].

2. Experimental procedure

CdS substrates used in this study were in the form of 2 mm thick wafers which were cut and polished with a basal-plane orientation. The crystals, their source, and method of preparation as substrates are described in the previous paper [1]. To ensure uniformity in the treatment of the two polar surfaces of CdS, each wafer was cut into two pieces and mounted side by side, exposing faces of opposite polarity. As indicated in the preceding paper, the basal planes of CdS in its wurtzite modification are composed alternately of sulphur and cadmium atoms exclusively. We refer to the (0001) or Cd and the ($000\bar{1}$) or S planes as the A and B faces, respectively.

Deposition of copper and gold films on the polar surfaces of CdS was carried out in an evaporation chamber with a base pressure of ~ 10^{-9} torr. Surface analysis and argon-ion sputter etching were carried out in an Auger electron spectroscopy (AES) system made by Physical Electronics. Details of the deposition and analysis processes are given in the previous paper [1].

3. Results and discussion

3.1. The Cu–CdS system

While the 920 eV copper peak is usually used for qualitative identification, the 60 eV peak was used in this study since it has a much higher surface sensitivity with a smaller Auger electron escape depth. A small amount of oxygen was observed in the AES spectra. Due to its low magnitude, however, it was not considered in the concentration calculations. A typical spectrum of copper on CdS is shown in Fig. 1.

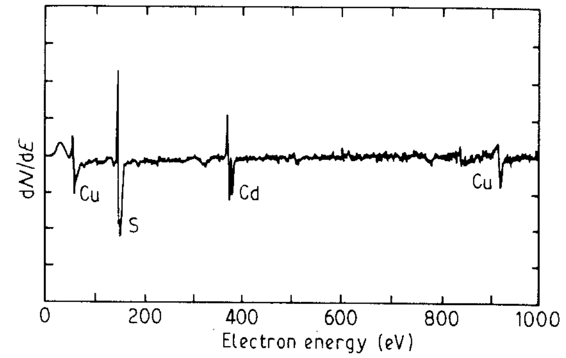

Figure 1 Typical Auger spectrum for Cu on CdS.

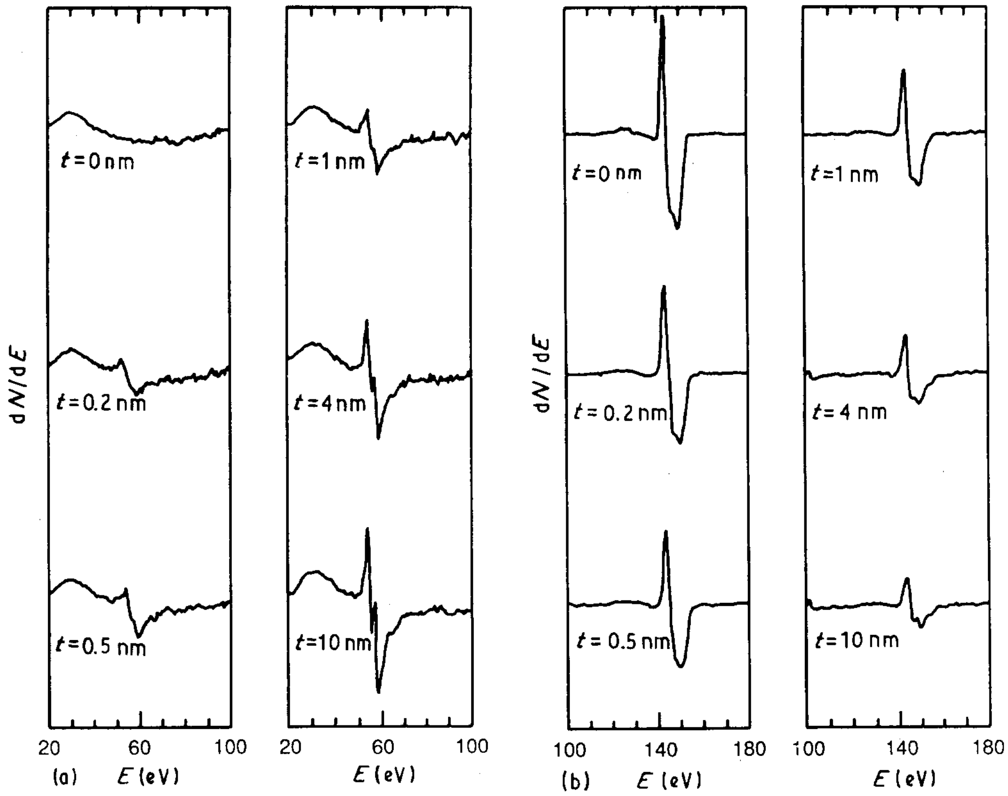

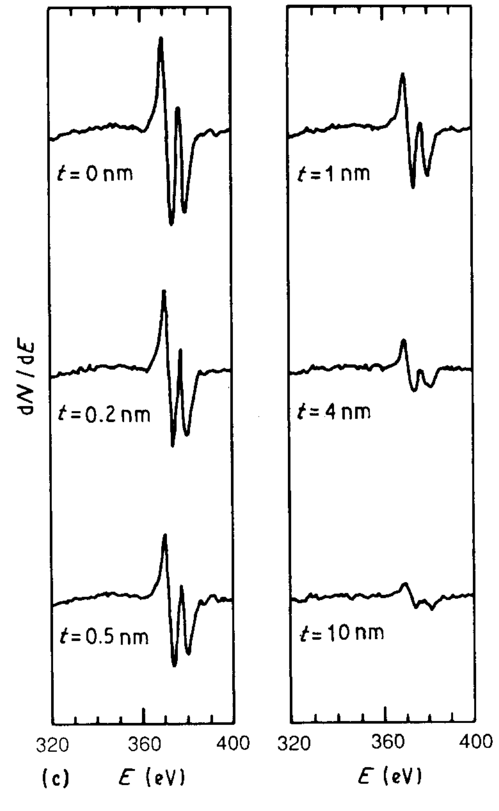

Figure 2 Peak shape and intensity as a function of Cu film thickness: (a) Cu peak, (b) S peak, (c) Cd peak.

The Cu *MNN* peak shifted to a lower energy region compared to the bulk position during the initial deposition. Coupled with a slight chemical shift of the S *LMM* peak towards a lower energy and the peak splitting at thick Cu coverages, these observations suggest the formation of Cu_2S. Since the difference in binding energy between Cu–Cu and Cu–S is much smaller than that between Al–Al and Al–S [1], only a small chemical shift of the Cu Auger peak was observed. The shift of Cd peaks toward higher energy again indicated the possibility of cation dissociation. The copper, sulphur and cadmium peak shapes and positions are given in Fig. 2a to c for different Cu film thicknesses.

The relationships between the concentrations of each component and the metal film thickness were very similar on both A and B faces and are demonstrated by Fig. 3 for the case of the A face of CdS. Significant out-diffusion of Cd and S into the copper occurred, since the peak intensities attenuate slowly with increasing metal coverage. The relative concentrations C/C_0 of Cd and S as a function of Cu coverage on CdS $\{0001\}$ (where C_0 is the concentration on clean surfaces) are shown in Fig. 4. The S/Cd peak height ratios decreased slightly during the initial metal deposition and then slowly increased for both faces. The similarity of the profiles for both the A face and the B face again indicated that the polarity did not play an important role in this system, as was observed in the case of Al films on CdS [1].

The initial small decrease in S/Cd concentration ratios as calculated from the data of Fig. 4 may be due to surface carbon contaminations. The subsequent increase in the ratio agrees with the concept of "chemical drawing" of the sulphur anions by the copper. However, when Cu and CdS are in contact, assuming that the dipole voltage determined by Brillson [4] at the cleavage surface is slightly modified due to the polarity and surface charge considerations for the basal planes, a negative dipole formed at the interface should induce a decrease in the S/Cd concentration ratio. Therefore, the metal–semiconductor dipole cannot account for the "chemical drawing" phenomenon.

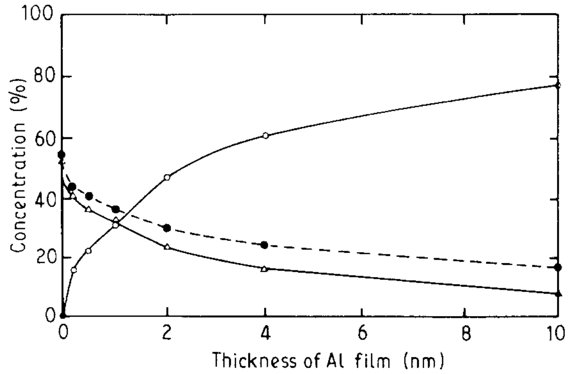

Figure 3 Surface concentrations of (○) Cu, (●) S and (△) Cd as a function of Cu coverage on (0 0 0 1) CdS.

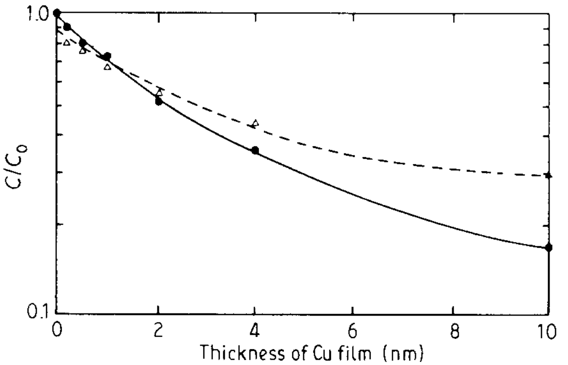

Figure 4 Relative concentrations of (●) Cd and (△) S as a function of Cu coverage on (0 0 0 1) CdS.

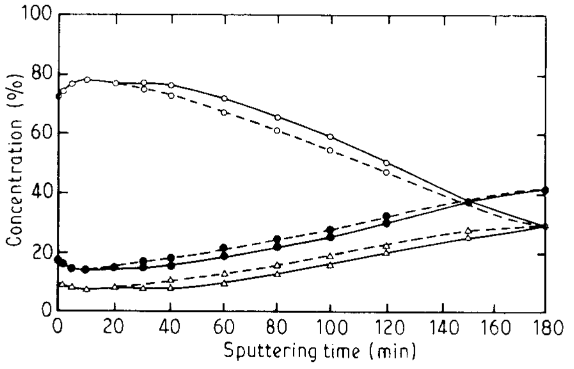

Figure 5 Surface concentrations of (○) Cu, (●) S and (△) Cd as a function of sputtering time on (——) (0 0 0 1) and (- - -) (0 0 0 $\bar{1}$) CdS.

Due to the relatively weak chemical reaction between Cu and S, no chemical trapping effect was observed. After leaving the samples overnight in the analysis chamber, both sulphur and cadmium concentrations increased slightly, indicating the continuous out-diffusion of both components. However, the S/Cd concentration ratios decreased slightly on both faces.

Only a slight amount of segregation of S and Cd to the free surfaces is indicated on the sputtering depth profiles shown in Fig. 5 for the A and B faces. By integrating the area under the Cu concentration curve as a function of sputtering time, an average sputtering rate is estimated to be $\sim 0.087\ \text{nm}\ \text{min}^{-1}$. The depth profiles revealed that semiconductor out-diffusion is continuous; both Cd and S compositions vary smoothly within the Cu overlayer, and the mixed Cu–Cd–S region can extend over tens of nanometres. This indicates not only that the components of CdS out-diffuse to the surface, but also that a great amount of Cu diffuses into the CdS substrate. From the data of Fig. 5, it is seen that the S/Cd ratios gradually decreased toward the bulk ratio as the metal layers were removed. Only a slight peak shift toward the positions of initial metal deposition was observed during the sputtering process, indicating the formation of Cu_2S at the original metal–semiconductor interface. The peak shapes and positions are shown in Fig. 6a to c.

3.2. The Au–CdS system

For reasons similar to those given for the selection of the Cu Auger peak, the 69 eV Au peak was used for the quantitative analysis instead of the 2024 eV peak. A typical gold on CdS spectrum is shown in Fig. 7. When comparing the spectrum of a pure gold standard with the spectrum of CdS it becomes evident that an overlap among the sulphur 152 eV peak and several gold minor peaks exists. This overlap caused a serious problem for quantitative calculations when the concentration of gold became much greater than sulphur as the gold film thickness was continuously increased. In order to measure the sulphur peak-to-peak height, a background gold spectrum was constructed by scaling the standard gold spectrum according to the ratio of the 69 eV peak-to-peak height in the collected spectrum and the standard spectrum. This background gold spectrum was then subtracted from the collected spectrum and the peak-to-peak height of sulphur and cadmium peaks was determined.

During the initial film build-up process, all the gold, sulphur and cadmium peaks shifted toward lower energies, as can be seen in Fig. 8a to c, with a slightly greater shift with the gold than with the sulphur peak. The cadmium peak had the least shift. The shifts increased as the thickness of the Au film increased and shifting stopped at about 2 nm thickness. The shifts were also greater on the A face than on the B face at the same thickness of the metal films.

The relationships between the concentration of each component and the metal film thickness are shown in Fig. 9 for the A and B faces. The relative concentrations C/C_0 of Cd and S as functions of Au coverages on CdS (0 0 0 1) are shown in Fig. 10. Again, the out-diffusion of both Cd and S components can be identified. The calculated S/Cd peak height ratios were nearly identical and decreased slightly as the gold film thickness increased. Since no chemical reaction was expected between Au and CdS, the non-stoichiometry of the semiconductor components in the Au overlayer was assumed to be caused by the dipole voltage at the metal–semiconductor interface. The cation-rich out-diffusion for Au interfaces with CdS single crystal agrees with the negative metal–semiconductor dipole formed at the interface as determined by Brillson [6] for cleaved CdS surfaces. However, the cadmium-rich out-diffusion is opposite to the preferential sulphur out-diffusion that Brillson observed on a cleaved CdS

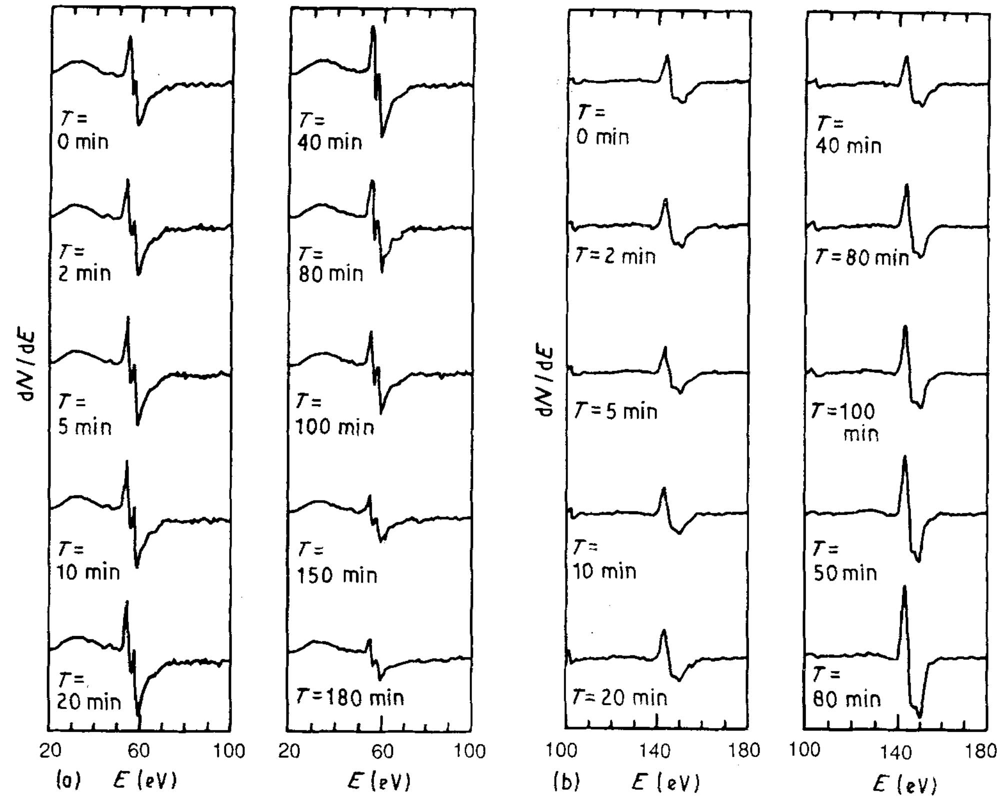

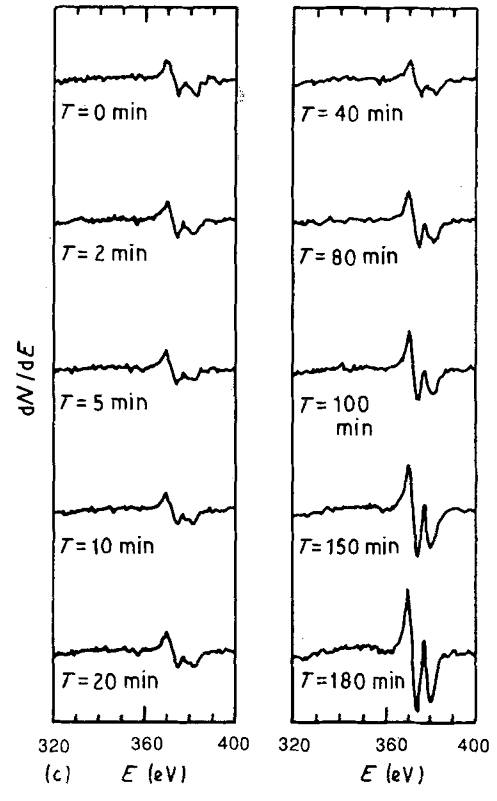

Figure 6 Peak shape and intensity as a function of sputtering time: (a) Cu peak, (b) S peak, (c) Cd peak.

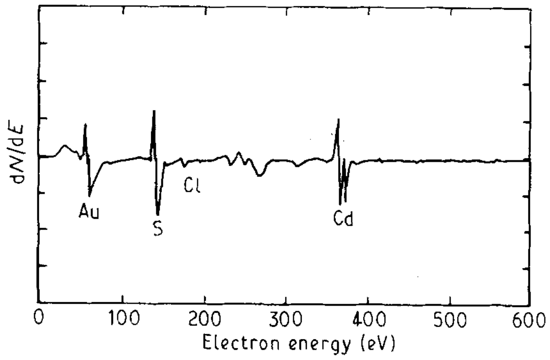

Figure 7 Typical Auger spectrum for Au on CdS.

surface. Also, higher concentrations of both sulphur and cadmium components were found on the B face, regardless of the expectation that the more negative dipole on the B face should enhance the out-diffusion of Cd and retard the out-diffusion of S. For a low-reactivity metal–semiconductor interface, this out-diffusion is not limited by any strong chemical reaction at the interface. Out-diffusion of Cd is expected for metals with high electronegativities such as Au, and the vacancies produced in the CdS could promote Au in-diffusion.

After the film thickness had reached 10 nm and the samples had been left overnight in the analysis chamber, Auger spectra were obtained and the peak-to-peak height measured as the films were removed by argon ion beam. The depth profiles of the concentrations versus sputtering time for the A and B faces are given in Fig. 11. By integrating the area under the Au concentration curve as a function of sputtering time, an average sputtering rate is estimated to be $\sim 0.136\ \mathrm{nm\,min^{-1}}$. The rather abrupt decrease in gold concentration at the interface indicates that the diffusion beyond the interface region is minimal. Strong surface segregation of both sulphur and cadmium components was observed. A sulphur and cadmium depletion region underneath the Au surface was noticed on both faces, which is also indirect evidence that the metal film was continuous at this

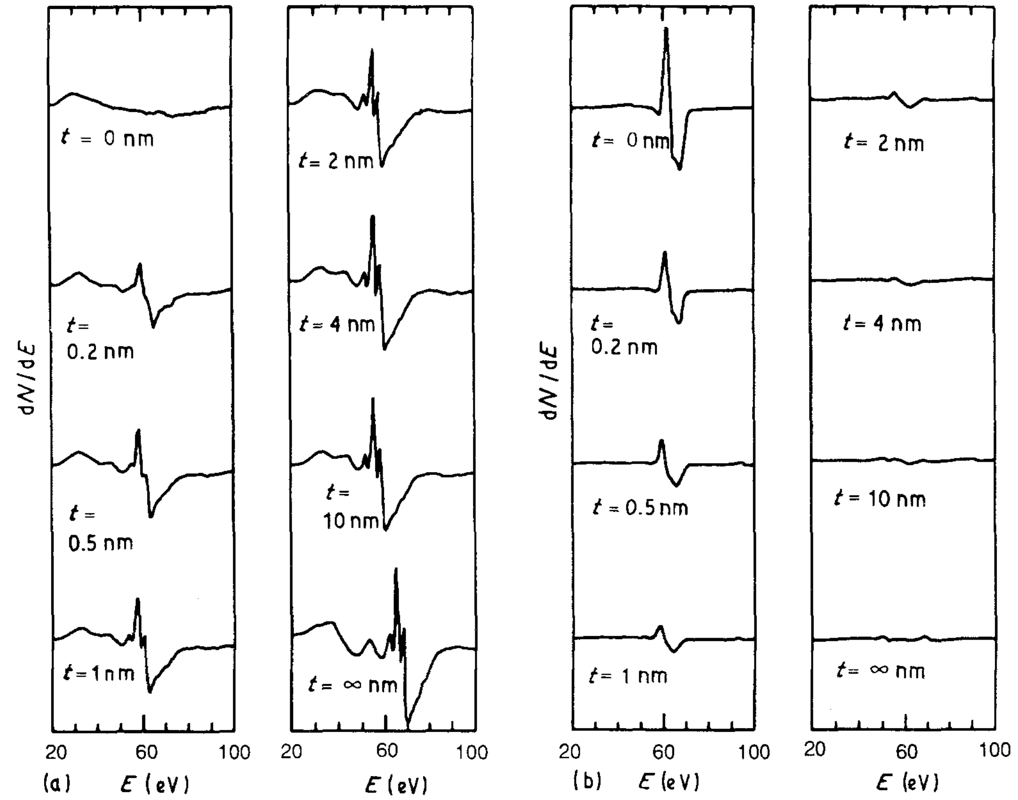

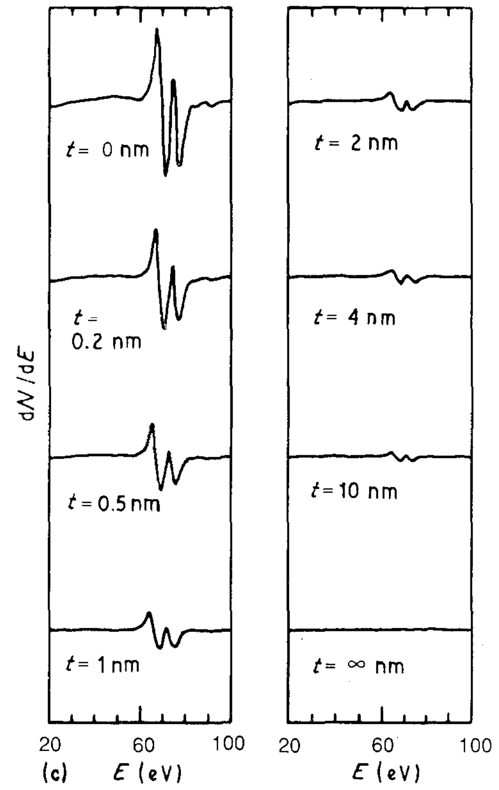

Figure 8 Peak shape and intensity as a function of sputtering time: (a) Au peak, (b) S peak, (c) Cd peak.

thickness. The depletion region was much greater on the A face than on the B face. The formation of the depletion region agrees with the low reactivity between Au and CdS, since any compound or alloy formed will show as a certain percentage of that element in the Au overlayer. Also, the observations of surface segregation and the depletion region underneath the Au surface indicate that the mixing of Au and CdS is thermodynamically unstable and the heat of mixing must be positive.

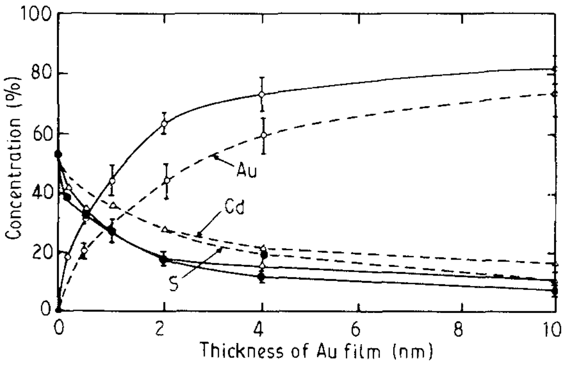

Figure 9 Surface concentrations of (○) Au, (●) S and (△) Cd as a function of Au coverage for (——) (0001) and (- - -) (000$\bar{1}$) CdS.

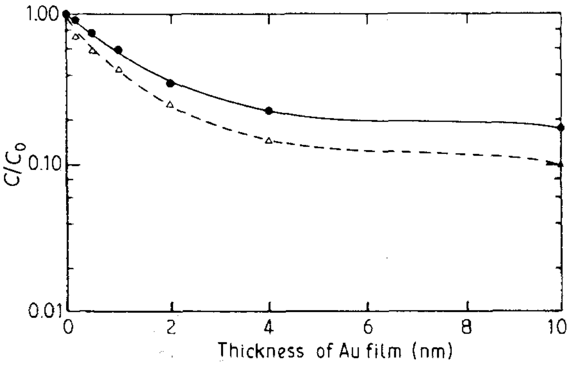

Figure 10 Relative concentrations of (●) Cd and (△) S as a function of Au coverage on (0001) CdS.

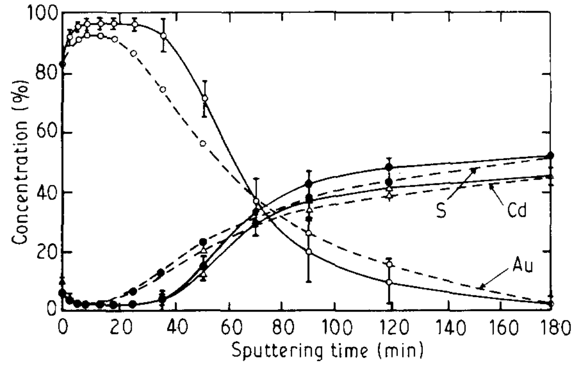

Figure 11 Surface concentrations of (○) Au, (●) S and (△) Cd as a function of sputtering time on (——) (0 0 0 1) and (- - -) ($0 0 0 \bar{1}$) CdS.

The S/Cd concentration ratios were calculated from the results shown in Fig. 11. Due to the small signal/noise ratios in the depletion region and the errors introduced from the peak deconvolution steps, the S/Cd concentration ratios were scattered in this region. Otherwise, no significant difference was found between the A and B faces.

During initial sputtering, due to the weak signals for the sulphur and cadmium peaks, their shifts could not be determined in this depletion region. However, as soon as the gold concentration started to decrease, all three peaks shifted back towards higher energies, opposite to the shifting to lower energies during the metal deposition process. Sulphur and cadmium peaks reached approximately the original positions when all the gold was removed. The peak positions and peak shapes at different sputtering times are shown in Fig. 12a to c.

Several possible mechanisms have been considered to explain the peak shifting for all the Auger peaks within the Au overlayer. Although no stable compound is formed, there may still exist an interfacial layer as in the Au–Si contact, which caused a marked change in the valence band features with the first few atomic layers of metal deposition [7]. Brillson [6] observed a continuous increase of the surface work function as the thickness of the gold film increased. This could also cause the Auger peaks to shift to lower energies; however, the shift is expected to be much smaller than what was observed. Another possibility is the formation of an insulating layer between the gold and CdS. When Au diffuses into the n-type CdS single crystal, the occupation of Cd lattice sites by the group-I Au atom results in the formation of a high-resistance layer near the surface where the concentration of Au atoms is great enough to remove most of the electrons from the conduction band. This could complicate the AES studies by a build-up of charge at the surface. If the secondary electron yield is less than unity, the surface potential is unstable due to the accumulation of negative charge, and it may reach rather high negative values. This would cause the Auger peaks to shift to higher energies in what is often termed "surface charging". However, a positive surface potential can develop when the secondary electron yield is greater than unity; a stable condition develops whereby low-energy secondaries can return to the sample, preventing excessive charging. The secondary electron yield can be rendered greater than unity by judicious choice of electron beam energy, angle of incidence of the electron beam, and temperature. Reducing the primary-beam incident angle from the usual 90° to between 20 and 45° with respect to the surface is most effective for insulators. When a stable positive surface potential is achieved, an Auger spectrum can be recorded, but the peaks will be shifted by between 2 and 15 eV towards lower energy [8]. Since the sample carousel in our system is at a 30° angle to the primary beam, the peak shifting may be due to this secondary electron effect.

Paterson *et al.* [9] showed that by using implanted, inert-gas-atom Auger peaks for energy referencing on charging substrates, a linear relationship was always found for plots of the energy of an Auger peak from any sample versus the energy of the Ar Auger peak. Generally, the slopes are near unity, indicating a uniform energy shift due to charge accumulation for all Auger peaks.

The Ar ion implanted during the sputter-etching process can be used as an energy reference; all the Au, S and Cd peaks shifted by about the same amount as the reference Ar peak, confirming the assumption that peak shifting was due to the charging of the crystal. However, peak shifting was not observed for the Cu–CdS system, where the formation of a similar high-resistivity layer was expected.

If we compare the peak shifting with the Au concentration profile, it seems that the shifting is strongly related to the surface concentration of Au. For example, in Fig. 8a to c, all the peaks shifted to lower energies up to about 2 nm thick Au film; as soon as the variation of the concentrations became small, the peaks shifting also slowed down. This indicates that the resistivity in the diffused layer increases as a function of the Au concentration until the surfaces become metal-like. This can also account for the differences in the amount of peak shifting between the two opposite polar surfaces, since a higher Au concentration was observed on the Cd face than on the S face.

3.3. Comparison of the different systems

Since no significant differences have been observed between the opposite polar surfaces of CdS, the following discussions are based on the Cd, or A, face and include the results presented in the previous paper [1].

Fig. 13 illustrates the S concentrations as a function of the metal overlayer coverage for Al, Cu, and Au on the CdS (0 0 0 1) face. The concentrations are normalized to the clean surface. The anion concentrations exhibit monotonic decreases with metal coverage which depend strongly on the particular metal–semiconductor combination. The strong initial attenuation of the anion concentrations for metal coverage argues against island formation in all cases. The stronger attenuation rate for the Al overlayer indicates the stronger chemical reaction between Al and S and a greater chemical trapping effect; the large attenuation rate for the Au overlayer may be due to the non-reactive interface and abrupt boundary, and the small

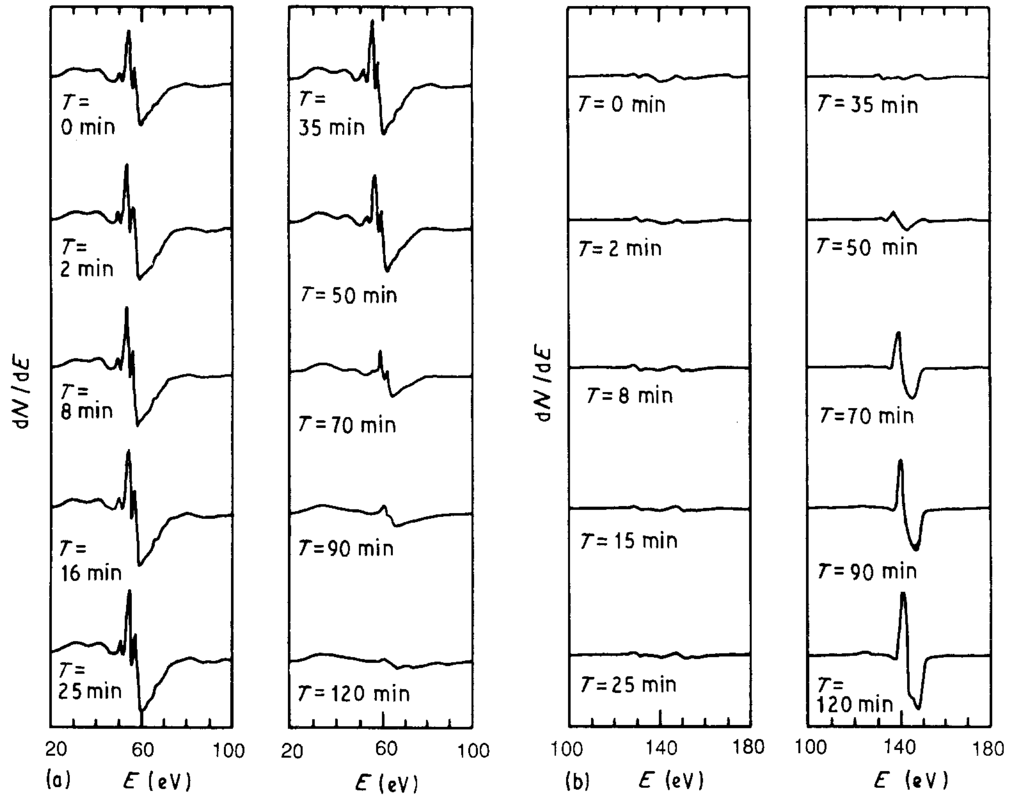

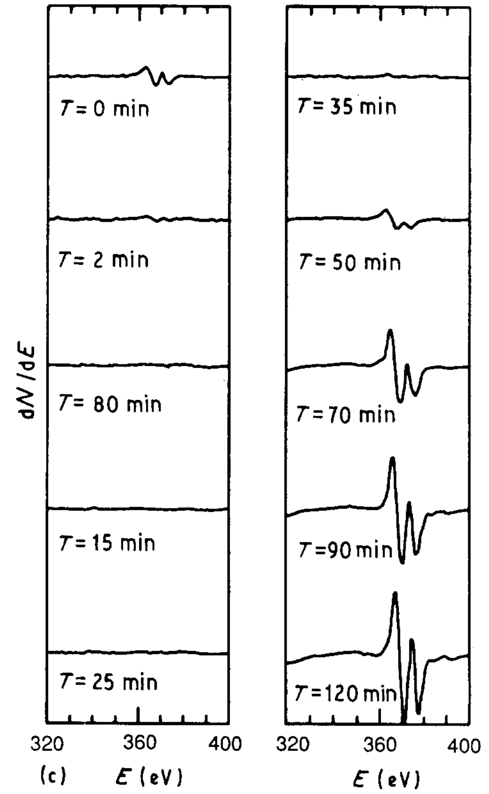

Figure 12 Peak shape and intensity as a function of sputtering time: (a) Au peak, (b) S peak, (c) Cd peak.

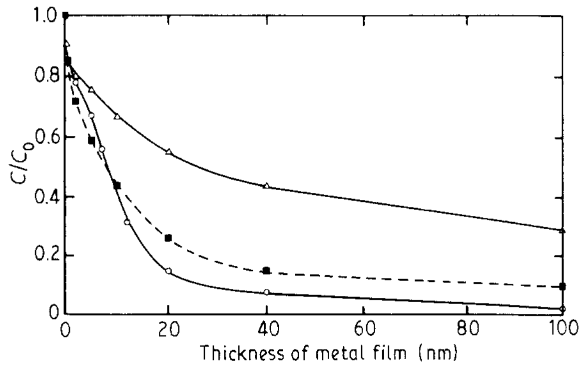

Figure 13 Relative surface concentrations of S as a function of metal coverage by (○) Al, (△) Cu and (■) Au.

attenuation rate for the Cu overlayer is probably due to the chemical drawing of the S anions out of the CdS substrate to the Cu overlayer.

The interface widths and the interface heats of reaction for the three metals (listed after each in nm and eV) are Al (1.0, − 1.4), Cu (7.5, 0.5), and Au (1.7, 3.9). The interface width is calculated as the metal overlayer thickness required to achieve anion attenuation by a factor 1/e. Because of the possible mixed metal–cation–anion bonding and chemical drawing, they do not show the same trend as in the III–V compounds [10]. Both the reactive metal (Al) and unreactive metal (Au) form abrupt junctions with CdS single crystal initially; however, due to the chemical reactions between the reactive metal and the semiconductor, as in the case of Al and CdS, the junctions can be extended to tens of nanometres with time, even at room temperature.

Fig. 14a demonstrates the out-diffusion as a function of metal film thickness for Al, Cu, and Au on CdS (0001). Au produces a nearly stoichiometric out-diffusion, Cu shows an anion-rich out-diffusion, and Al shows a cation-rich out-diffusion at thick metal layers. These results are similar to those for metal films on III–V compounds reported by Brillson *et al.* [11]. The anion-rich out-diffusion for Al at thin metal coverage may be due to the chemical drawing of the sulphur anions by the metal.

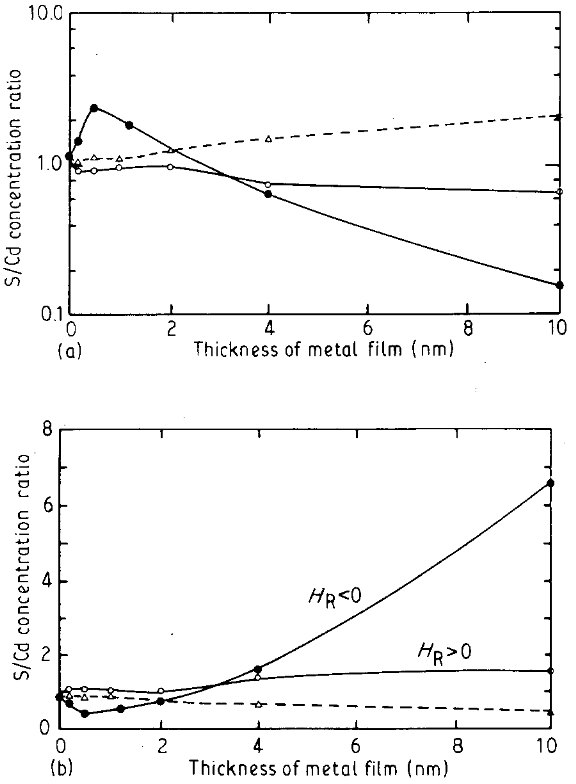

Figure 14 (a) S/Cd concentration ratios as a function of metal coverage for (●) Al, (△) Cu and (○) Au films. (b) S/Cd concentration ratios as a function of metal film thickness, showing delineation between reactive and non-reactive regimes.

The cation/anion concentration ratios as a function of metal film thickness (Fig. 14b) illustrates a clear delineation between reactive ($\Delta H_R < 0$) and unreactive ($\Delta H_R > 0$) regimes (where ΔH_R refers to enthalpy of formation of the metal–anion compound). However, the general trend does not agree with the corresponding curves reported for cleaved surfaces [12].

Because the dipole voltage did not play an important role in any of the three metal–semiconductor systems, the variation of the concentration profiles for Al–CdS and Cu–CdS systems are believed to be caused solely by the chemical effect. Since the chemical reactions are expected to be very similar between reactive metals and compound semiconductors, regardless of whether the semiconductor is a III–V or II–VI compound, a possible mechanism can be proposed. When a reactive metal, such as Al, is deposited on to the surface of CdS, due to the strong chemical reaction between Al and S, the sulphur anions will be drawn chemically to the metal layer, causing the increase of S/Cd concentration ratio. As the metal film thickness increases, the sulphur anions have to be drawn from the bulk crystal to the metal–semiconductor interface, then through the reacted layer to the surface. If either one of these two processes is slow, the supply of the sulphur anions to the surface will be limited, and the S/Cd concentration ratio is reduced. This mechanism, which suggests that both "chemical trapping" and "chemical drawing" effects are the same, may apply to both III–V and II–VI compound semiconductors.

4. Conclusions

1. Reactive out-diffusion of sulphur into the copper layer resulted in a broad interfacial boundary. However, because of the relatively weak chemical bonding between sulphur and copper, no chemical trapping effect was observed.

2. Gold forms a high-resistivity layer at the CdS interface, causing a shift in the Auger peaks. The interface dipole voltage induced by the Au deposition may account for the Cd-rich out-diffusion in the Au overlayer.

3. The non-stoichiometric out-diffusion of sulphur and cadmium for the Cu and Au films (as well as the aluminium films reported in the previous paper [1]) is similar to the case of films of these metals on III–V compounds. The cation/anion concentration ratios as functions of metal film thickness show a clear delineation between reactive and non-reactive metals.

4. As was the case for the Al–CdS system [1], there was no difference in behaviour between the A (0001) and B $(000\bar{1})$ faces of CdS. This raises the question of whether electromigration played a role in the interface diffusion, especially in the Au–CdS system where no chemical reaction is expected.

5. Interfacial bonding at the microscopic level plays a central role in the process of interdiffusion. Differences in observations made in this study and in previously reported investigations may be due to differences in crystal orientation of the CdS substrate or to surface preparation methods.

Acknowledgements

This work was supported by a grant from the Ceramics and Electronic Materials Program, Division of Materials Research, The National Science Foundation.

References

1. E. K. CHIEH and Z. A. MUNIR, *J. Mater. Sci.* in press.
2. L. J. BRILLSON, *Surf. Sci. Repts* **2** (1982) 123.
3. *Idem*, *J. Vac. Sci. Technol.* **16** (1979) 1137.
4. *Idem*, *Phys. Rev.* **B18** (1978) 2431.
5. C. F. BRUCKER and L. J. BRILLSON, *J. Vac. Sci. Technol.* **18** (1981) 787.
6. L. J. BRILLSON, *ibid.* **15** (1978) 1378.
7. L. BRAICOVICH, C. M. GARNER, P. R. SKEATH, C. Y. SU, P. W. CHYE, I. LINDAU and W. E. SPICER, *Phys. Rev.* **B20** (1979) 5131.
8. M. THOMPSON, M. BAKER, A. CHRISTIE and J. TYSON, *Chem. Anal.* **74** (1985) 93.
9. J. K. PATERSON, P. H. HOLLOWAY and Y. E. STRAUSSER, *Appl. Surf. Sci.* **4** (1980) 37.
10. L. J. BRILLSON, C. F. BRUCKER, N. G. STOFFEL, A. D. KATNANI and G. MARGARITONDO, *Phys. Rev. Lett.* **46** (1981) 838.
11. L. J. BRILLSON, C. F. BRUCKER, A. D. KATNANI, N. G. STOFFEL and G. MARGARITONDO, *Appl. Phys. Lett.* **38** (1981) 784.
12. C. F. BRUCKER and L. J. BRILLSON, *J. Vac. Sci. Technol.* **19** (1981) 617.

Received 30 March
and accepted 19 November 1990